7th European Conference on Structural Dynamics
EURODYN 2008
7-9 July 2008 Southampton

# ON FINITE ELEMENT METHODS FOR NONLINEAR DYNAMIC RESPONSE

**Klaus-Jürgen Bathe**

Massachusetts Institute of Technology
Cambridge, MA 02139, U.S.A.

## ABSTRACT

In this paper we briefly focus on the nonlinear analysis of solids and structures when these undergo large deformations, possibly over long time durations, and perhaps subjected to fluid-structure interactions. The analysis should be conducted with finite element methods, including the time integration, that are reliable and effective. The requirement of reliability is particularly important in nonlinear finite element analysis because physical test data are frequently not available.

## 1. INTRODUCTION

Finite element methods are now widely used in engineering analysis and we can expect a continued growth in the use of these methods. Finite element programs are extensively employed for linear and nonlinear analyses, and the simulations of highly nonlinear events are of much interest [1-3].

An important point is that for large civil and mechanical engineering structures like long-span bridges, offshore platforms, storage tanks and power plants, physical tests can only be performed to a limited extent. Parts of the structures can be tested but a complete actual structure can only be tested when entirely assembled in the field, and sometimes that is not possible either. Hence, the results of simulations of such structures cannot be compared with test data. It is then very important to use reliable finite element methods in order to have the highest possible confidence in the computed results [3].

The objective in this paper is to survey some finite element techniques for nonlinear dynamic analysis with a particular focus on the reliability of the methods. Of course, any simulation starts with the selection of a mathematical model, and this model must be chosen judiciously. However, once an appropriate mathematical model has been selected, for the questions asked, the finite element solution of that model needs to be obtained reliably, effectively, and ideally to a controlled accuracy.

In the following sections we briefly consider the solution of problems involving 2D and 3D solids, plates and shells, including fluid-structure interactions, undergoing large dynamic deformations. First we discuss some appropriate techniques for solution and then we give some illustrative example solutions. This brief exposition is an update of Ref. [4], with some parts abridged and other parts expanded.

## 2. ON THE SELECTION OF THE MATHEMATICAL MODEL

The first step of any analysis is the selection of an appropriate mathematical model [3]. This model needs to be chosen based on the analysis questions asked. Of course, the model is based on the selection of the geometry, material properties, the loading and boundary conditions, and any other specific assumptions made.

The purpose of the analysis is to answer certain questions regarding the stiffness, stresses developed and strength of the structure. Hence, when studying the behavior of the structure, we would like to predict the future not only when the structure is operating in normal conditions, which mostly only requires a linear analysis, but also when the structure is subjected to severe loading conditions, which usually requires a highly nonlinear analysis.

It is clear that the finite element solution of the mathematical model will contain all the assumptions of the mathematical model and hence cannot predict any response not contained in this model. Selecting the appropriate mathematical model is therefore a most important step of the analysis. A fundamental question is then always whether the mathematical model used is appropriate. This question can be addressed by the process of hierarchical modeling, which involves the solution of a number of hierarchically more encompassing mathematical models [3]. However, such solutions can result in high costs and are at present hardly performed in engineering practice.

In the following we only consider deterministic analyses. But the considerations given here are all valid because the deterministic procedures are basic methods used in non-deterministic analyses as well [1].

## 3. THOUGHTS ON THE RELIABILITY OF FINITE ELEMENT METHODS

With the mathematical model chosen, finite element procedures are used to solve the model. It is important that well-founded and reliable methods be used. By reliability of a finite element procedure we mean that in the solution of a well-posed mathematical model, the procedures always, for a reasonable finite element mesh, give a reasonable solution. And if the mesh is reasonably fine, an accurate solution of the chosen mathematical model is obtained [3].

It is sometimes argued that since the geometry, material properties, loadings are not known to great accuracy, there is no need to solve the mathematical model accurately. This is a reasonable argument provided the mathematical model is solved to 'sufficient' accuracy *and* a proper control on the level of accuracy is calculated. Such a control on the accuracy of the finite element solution of the mathematical model is difficult to achieve, in particular when the level of accuracy sought is low, and reliable finite element procedures are best used.

The reliability of a finite element procedure means in particular that when some geometric or material properties are changed in the mathematical model, then for a given finite element mesh the accuracy of the finite element solution does not drastically decrease. Hence, pure displacement-based finite element methods are not reliable when considering almost incompressible materials (like a rubber material, or a steel in large strains). As is well known, these methods 'lock', and for such analyses, well-founded mixed methods are best used [3].

To exemplify what can go wrong in a finite element solution when unreliable finite element procedures are used, we refer to Ref. [3], page 474, where the computed frequencies of a cantilever bracket are given. With reduced integration phantom frequencies that are non-physical are predicted. Such ghost frequencies may also be predicted when some hourglass control with reduced integration is employed.

Similar situations arise in the analysis of plates and shells and in the analyses of fluids and fluid-structure interactions, but there are important additional considerations, as discussed briefly in the following sections.

Considering transient analysis, in addition to the finite element formulations for the spatial discretizations, also the time integration scheme should be reliable and effective. Here, we

describe an implicit method that is unconditionally stable (in the traditional sense), and even remains stable in long time duration large deformation response, and does so without adjustable parameters.

## 4. THE ANALYSIS OF SOLIDS AND STRUCTURES

The use of well-formulated mixed methods has greatly enhanced the reliable analysis of solids and structures [3].

Considering the analysis of solids, in large strains, the condition of an almost incompressible material response is frequently reached. This situation is encountered in simulations involving rubber-like materials and inelastic conditions, like elasto-plasticity and visco-plasticity. In these analyses, the displacement/pressure (u/p) finite elements are very effective. An optimal element uses for a given displacement interpolation the highest pressure interpolation that satisfies the inf-sup condition [3,5,6]

$$\inf_{q_h \in Q_h} \sup_{\mathbf{v}_h \in V_h} \frac{\left(q_h, \operatorname{div} \mathbf{v}_h\right)}{\left\|q_h\right\|_0 \left\|\mathbf{v}_h\right\|_1} \geq \beta > 0 \tag{1}$$

where $V_h$ is the finite element displacement space, $Q_h$ is the finite element pressure space, and $\beta$ is a constant independent of $h$ (the element size). Reference [3] gives a table of u/p elements that satisfy the above inf-sup condition, see also Ref. [5]. For example, for 2D solutions the element based on 9 nodes for the displacement interpolations and 3 internal degrees of freedom for the pressure interpolation is optimal. But, in practice, a 4-node element is desirable and frequently the 4/1 element (4 nodes for the displacement interpolations and a constant pressure) is used. While the 4/1 element does not satisfy the above inf-sup condition, it can be quite effective when used with care. A 4-node element that does satisfy the inf-sup condition was presented by Pantuso and Bathe [7] but is much more expensive and does not perform sufficiently well in nonlinear large strain analysis. Equivalent elements exist for 3D solutions.

In the analysis of plates and shells, the situation is much more complex Here, for a given mesh, an optimal element would give the same error irrespective of the thickness of the plate or shell, and that for any plate and shell geometry, boundary conditions and admissible loading used [3,8]. As is well known, the displacement-based shell elements formulated using the Reissner-Mindlin kinematic assumption are not effective in the analysis of general shells, and for this reason research has focused on the development of mixed elements, based in essence on the general formulation:

Find $\boldsymbol{u}_h \in V_h$ and $\boldsymbol{\xi}_h \in E_h$

$$a\left(\mathbf{u}_h, \mathbf{v}_h\right) + b\left(\boldsymbol{\xi}_h, \mathbf{v}_h\right) = f\left(\mathbf{v}_h\right) \quad \forall\, \mathbf{v}_h \in V_h \tag{2}$$

$$b\left(\boldsymbol{\eta}_h, \mathbf{u}_h\right) - t^2 c\left(\boldsymbol{\eta}_h, \boldsymbol{\xi}_h\right) = \mathbf{0} \quad \forall\, \boldsymbol{\eta}_h \in E_h \tag{3}$$

where $a(\cdot,\cdot)$, $b(\cdot,\cdot)$, and $c(\cdot,\cdot)$, are bilinear forms, $f(\cdot)$ is a linear form, $t$ is the thickness of the shell, and $V_h$ , $E_h$ are the finite element displacement and strain spaces.

Mixed elements, however, then should satisfy the consistency condition, the ellipticity condition, and ideally the inf-sup condition [5,6,8]

$$\sup_{\mathbf{v}_h \in V_h} \frac{b\left(\boldsymbol{\eta}_h, \mathbf{v}_h\right)}{\left\|\mathbf{v}_h\right\|_V} \geq c \sup_{\mathbf{v} \in V} \frac{b\left(\boldsymbol{\eta}_h, \mathbf{v}\right)}{\left\|\mathbf{v}\right\|_V} \quad \forall\, \boldsymbol{\eta}_h \in E_h \tag{4}$$

where $V$ is the complete (continuous) displacement space, and $c$ is a constant, greater than zero, independent of $t$ and $h$. To show analytically that the inf-sup condition is satisfied for an element is very difficult because it involves the complete space $V$.

If an element satisfies these conditions, the discretization is optimal in all shell analyses, that is, in the analyses of membrane-dominated shells, bending-dominated shells, and mixed-behavior shells. For the membrane-dominated case, the displacement-based shell elements perform satisfactorily but for the bending-dominated and mixed cases, the displacement-based elements 'lock' and a mixed formulation need be used — which satisfies the consistency, ellipticity, and ideally the inf-sup condition. The inf-sup condition can actually be by-passed, but then nonphysical numerical factors enter the element formulation [8].

The first mixed shell elements, introduced some decades ago, were not tested for these conditions, and only relatively lately a more rigorous testing has been proposed [8,9]. Here, instead of testing directly whether the expression (4) holds, suitable benchmark test problems are used to identify whether the inf-sup condition is satisfied. The mixed-interpolated-tensorial-components (MITC) shell elements, see Refs. [3,8,10] and the references therein, have performed quite well in these test cases. Indeed, the MITC4 shell element (the 4-node element [3]) has shown excellent convergence behavior and is used abundantly in a number of finite element codes.

The MITC interpolations can of course also be employed in the formulation of 3D-shell elements [11]. Here the shell is described as a solid with stresses and strains measured through the shell thickness, and possibly higher assumptions for the in-plane components as well. Shear, membrane and pinching locking effects need then to be circumvented, and this can be achieved quite effectively using the MITC interpolations. In addition, ill-conditioning must be prevented.

## 5. THE ANALYSIS OF CONTACT CONDITIONS

An analysis area in which, recently, still considerable advances have taken place, is the solution of contact problems, including frictional effects. The aim is to reach more accuracy, in particular when higher-order elements are used. The higher-order elements are typically 10-node or 11-node 3D tetrahedral elements generated in free-form meshing. For such analyses, the consistent solution algorithm proposed in Ref. [12] is valuable in that the patch test can be satisfied exactly. The algorithm is also used effectively in glueing together different meshes, in usual complex analyses and possibly multi-scale solutions.

The basic approach is that along the contactor surface, the tractions are interpolated and the gap and slip between the contactor and target are evaluated from the nodal positions and displacements. Let $\lambda(s)$ be the contact pressure and $g(s)$ be the gap at the position $s$ along the contact surface $\Gamma_C$, then the normal contact conditions are

$$g \geq 0, \quad \lambda \geq 0, \quad g\lambda = 0 \tag{5}$$

where the last equation in (5) is the complementary condition. We use a constraint function $w_n(g,\lambda)$ to turn the inequality constraints of contact into the equality constraint

$$w_n(g,\lambda) = 0 \tag{6}$$

which gives in variational form

$$\int_{\Gamma_C} w_n(g,\lambda)\,\delta\lambda \, \mathrm{d}\Gamma_C = 0 \tag{7}$$

Whether the gap is open or closed on the surface is automatically contained in the formulation using the constraint function.

The scheme published in Ref. [12] should be used with appropriate interpolations for the contact pressure — for given geometry and displacement interpolations — and appropriate numerical integration schemes to evaluate the integrals enforcing the contact conditions.

The inf-sup condition for the contact discretization is given by

$$\sup_{\mathbf{v}_h \in V_h} \frac{\int_{\Gamma_C} \mu_h g(\mathbf{v}_h)\, \mathrm{d}\Gamma_C}{\|\mathbf{v}_h\|_1} \geq \beta \sup_{\mathbf{v} \in V} \frac{\int_{\Gamma_C} \mu_h g(\mathbf{v})\, \mathrm{d}\Gamma_C}{\|\mathbf{v}\|_1} \quad \forall \mu_h \in M_h \tag{8}$$

where $M_h$ is the space of contact tractions and $\beta$ is a constant, greater than zero. This condition can be satisfied by appropriate choices of interpolations.

Above, we considered the normal contact condition. For the tangential conditions we have the governing equations

$$\left.\begin{aligned} \tau &= \frac{t}{\mu\lambda} \\ |\tau| &\leq 1 \\ |\tau| < 1 &\text{ implies } \dot{u} = 0 \\ |\tau| = 1 &\text{ implies } \operatorname{sign}(\dot{u}) = \operatorname{sign}(\tau) \end{aligned}\right\} \tag{9}$$

where $t$ is the tangential traction, $\dot{u}$ is the tangential relative velocity and $\mu$ is the friction coefficient. These conditions are also imposed using a constraint function, see Ref. [3].

## 6. THE ANALYSIS OF FLUID-STRUCTURE INTERACTIONS

The analysis of fluid-structure interactions (FSI) has attracted, in recent years, much attention because the dynamic behavior of structures can be greatly affected by surrounding fluids. If the fluid can be idealized as an acoustic fluid (inviscid, irrotational and undergoing only small motions), the analysis is much simpler than when actual flow with Euler or Navier-Stokes fluid assumptions are considered.

Some finite element representations of an acoustic fluid are simple extensions of solid analysis discretizations, assuming a large bulk modulus and a very small shear modulus (corresponding to the fluid viscosity). However, these fluid models are not effective because they can 'lock' and lead to the usual unreliability when 'reduced' integration is used (see above), and have in 3D analysis three displacement degrees of freedom per node. Even when formulated in a mixed formulation, a difficulty is to prevent loss of mass. In addition, the formulations may then contain many zero energy modes, or modes of very small energy [13].

A clearly more effective approach is to use a potential formulation [3]. Such formulation extended also for actual flow has been used very successfully to solve large and complex fluid-structure interactions [14].

Considering Navier-Stokes fluids, the solution requires effective discretizations to model the fluid including high Péclet and Reynolds number conditions, effective finite element methods for the structure, and the proper coupling of the discretizations.

We have concentrated our development efforts on establishing finite element discretization schemes for the fluid that are stable, even when coarse meshes are used for very high (element) Péclet and Reynolds numbers and show good accuracy [15,16]. The basic approach is to use the velocity-pressure interpolations to satisfy the incompressibility inf-sup condition, flow-condition-based interpolations (FCBI) in the convective terms of the fluid, and to use

element control volumes (like in the finite volume method) to assure local mass and momentum conservation.

To briefly summarize the essence of the FCBI formulation, consider the solution of the following Navier-Stokes equations governing steady-state conditions:

Find the velocity $\mathbf{v}(\mathbf{x}) \in V$ and the pressure $p(\mathbf{x}) \in P$ in the domain $\Omega$ such that

$$\nabla \cdot \mathbf{v} = 0, \quad \mathbf{x} \in \Omega \tag{10}$$

$$\nabla \cdot \left( \rho \mathbf{v}\mathbf{v} - \boldsymbol{\tau} \right) = \mathbf{0}, \quad \mathbf{x} \in \Omega \tag{11}$$

$$\boldsymbol{\tau} = \boldsymbol{\tau}\left( \mathbf{v}, p \right) = -p\mathbf{I} + \mu \left\{ \nabla \mathbf{v} + \left( \nabla \mathbf{v} \right)^{\mathrm{T}} \right\} \tag{12}$$

where we assume that the problem is well-posed in the Hilbert spaces $V$ and $P$, $\boldsymbol{\tau}$ is the stress tensor, $\rho$ is the density and $\mu$ is the viscosity. Equations (10) and (11) are subject to appropriate boundary conditions.

In the FCBI approach, we use for the solution a Petrov-Galerkin variational formulation with subspaces $U_h$, $V_h$, and $W_h$ of $V$, and $P_h$ and $Q_h$ of $P$. The formulation for the numerical solution is:

Find $\mathbf{u}_h \in U_h$, $\mathbf{v}_h \in V_h$ and $p_h \in P_h$ such that for all $w \in W_h$ and $q \in Q_h$

$$\int_\Omega w \nabla \cdot \left( \rho \mathbf{u}_h \mathbf{v}_h - \boldsymbol{\tau}\left( \mathbf{u}_h, p_h \right) \right) \mathrm{d}\Omega = \mathbf{0} \tag{13}$$

$$\int_\Omega q \nabla \cdot \mathbf{u}_h \, \mathrm{d}\Omega = 0 \tag{14}$$

The trial functions in $U_h$ and $P_h$ are the usual functions of finite element interpolations for velocity and pressure, respectively. But an important point is that the trial functions in $V_h$ are different from the functions in $U_h$ and are defined using the flow conditions in order to stabilize the convection term. The functions in the spaces $W_h$ and $Q_h$ are step functions and enforce the local conservation of momentum and mass, respectively.

The resulting FCBI elements do not require a tuning of upwind parameters, satisfy the property of local and global mass and momentum conservation, pass the inf-sup test of incompressible analysis and appropriate patch tests on distorted meshes. Also, the interpolations can be used to establish consistent Jacobian matrices for the iterations in the incremental step-by-step solutions. We have developed these elements for incompressible, slightly compressible and low-speed compressible steady-state and transient flows. Each of these flow categories are abundantly used in engineering practice with various turbulence models. Of course, we continue our research to improve the FCBI formulations [17]. However, for high-speed compressible flows we employ the widely used Roe scheme.

These fluid flow models can all be coupled in an arbitrary Lagrangian-Eulerian formulation with structural models, in large deformations, with contact conditions [18,19] and, if considered, piezo-electric, thermal and electro-magnetic effects.

## 7. THE TIME INTEGRATION

Consider that an appropriate finite element model and the governing algebraic equations have been established for a nonlinear dynamic analysis. The next step is to time-integrate the governing finite element equilibrium equations.

If the response is of short duration, the explicit central difference time integration scheme is used and is probably most effective. However, in central differencing the integration time step must usually be very small, for stability. For analyses involving longer time durations, implicit time integration can be much more effective.

Considering transient structural response, a widely used scheme of time integration is the Newmark method trapezoidal rule. However, if large deformations over long-time durations need be solved, this scheme can be unstable and the scheme given in Ref. [20] can be much more effective. Consider that the solution at time $t$ has been established and that the solution at time $t + \Delta t$ shall be obtained. The governing equations for a structural model to be solved are then

$$\mathbf{M}\,{}^{t+\Delta t}\ddot{\mathbf{U}} + \mathbf{C}\,{}^{t+\Delta t}\dot{\mathbf{U}} = {}^{t+\Delta t}\mathbf{R} - {}^{t+\Delta t}\mathbf{F} \tag{15}$$

where **M** is the mass matrix, **C** is the damping matrix, **R** is the vector of externally applied loads, **F** is the vector of nodal forces equivalent to the element stresses, and **U** denotes nodal displacements (including rotations). The superscript $t + \Delta t$ denotes of course time and an overdot a time derivative.

In the time integration scheme of Ref. [20] we consider each time step $\Delta t$ to consist of two equal sub-steps, each solved implicitly. The first sub-step is solved using the trapezoidal rule with the usual assumptions

$${}^{t+\Delta t/2}\dot{\mathbf{U}} = {}^{t}\dot{\mathbf{U}} + \left[\frac{\Delta t}{4}\right]\left({}^{t}\ddot{\mathbf{U}} + {}^{t+\Delta t/2}\ddot{\mathbf{U}}\right) \tag{16}$$

$${}^{t+\Delta t/2}\mathbf{U} = {}^{t}\mathbf{U} + \left[\frac{\Delta t}{4}\right]\left({}^{t}\dot{\mathbf{U}} + {}^{t+\Delta t/2}\dot{\mathbf{U}}\right) \tag{17}$$

and the second sub-step is solved using the three-point Euler backward method with the governing equations

$${}^{t+\Delta t}\dot{\mathbf{U}} = c_1\,{}^{t}\mathbf{U} + c_2\,{}^{t+\Delta t/2}\mathbf{U} + c_3\,{}^{t+\Delta t}\mathbf{U} \tag{18}$$

$${}^{t+\Delta t}\ddot{\mathbf{U}} = c_1\,{}^{t}\dot{\mathbf{U}} + c_2\,{}^{t+\Delta t/2}\dot{\mathbf{U}} + c_3\,{}^{t+\Delta t}\dot{\mathbf{U}} \tag{19}$$

where $c_1 = 1/\Delta t$, $c_2 = -4/\Delta t$, $c_3 = 3/\Delta t$.

Using the Newton-Raphson iteration, the full solution algorithm for a time step is therefore as follows.

We solve for $i = 1, 2, 3, \ldots$

$$\begin{aligned}
&\left(\frac{16}{\Delta t^2}\mathbf{M} + \frac{4}{\Delta t}\mathbf{C} + {}^{t+\Delta t/2}\mathbf{K}^{(i-1)}\right)\Delta\mathbf{U}^{(i)} \\
&= {}^{t+\Delta t/2}\mathbf{R} - {}^{t+\Delta t/2}\mathbf{F}^{(i-1)} \\
&\quad - \mathbf{M}\left(\frac{16}{\Delta t^2}\left({}^{t+\Delta t/2}\mathbf{U}^{(i-1)} - {}^{t}\mathbf{U}\right) - \frac{8}{\Delta t}\,{}^{t}\dot{\mathbf{U}} - {}^{t}\ddot{\mathbf{U}}\right) \\
&\quad - \mathbf{C}\left(\frac{4}{\Delta t}\left({}^{t+\Delta t/2}\mathbf{U}^{(i-1)} - {}^{t}\mathbf{U}\right) - {}^{t}\dot{\mathbf{U}}\right)
\end{aligned} \tag{20}$$

where

$$ {}^{t+\Delta t/2}\mathbf{U}^{(i)} = {}^{t+\Delta t/2}\mathbf{U}^{(i-1)} + \Delta\mathbf{U}^{(i)} \tag{21} $$

Once convergence has been reached, we use the calculated displacements ${}^{t+\Delta t/2}\mathbf{U}$ with Eqs. (16) and (17) to obtain the velocities (and accelerations) at time $t + \Delta t/2$.
Then in the second sub-step, we solve Eqs. (15) with the equations of the three-point Euler backward method

$$ {}^{t+\Delta t}\dot{\mathbf{U}} = \frac{1}{\Delta t}{}^{t}\mathbf{U} - \frac{4}{\Delta t}{}^{t+\Delta t/2}\mathbf{U} + \frac{3}{\Delta t}{}^{t+\Delta t}\mathbf{U} \tag{22} $$

$$ {}^{t+\Delta t}\ddot{\mathbf{U}} = \frac{1}{\Delta t}{}^{t}\dot{\mathbf{U}} - \frac{4}{\Delta t}{}^{t+\Delta t/2}\dot{\mathbf{U}} + \frac{3}{\Delta t}{}^{t+\Delta t}\dot{\mathbf{U}} \tag{23} $$

Using these equations and the earlier solutions obtained for time $t + \Delta t/2$, the governing equations for the Newton-Raphson iteration to solve Eqs. (15) are for $i$=1, 2, 3, …

$$ \begin{aligned} &\left(\frac{9}{\Delta t^2}\mathbf{M} + \frac{3}{\Delta t}\mathbf{C} + {}^{t+\Delta t}\mathbf{K}^{(i-1)}\right)\Delta\mathbf{U}^{(i)} \\ &= {}^{t+\Delta t}\mathbf{R} - {}^{t+\Delta t}\mathbf{F}^{(i-1)} \\ &- \mathbf{M}\left(\frac{9}{\Delta t^2}{}^{t+\Delta t}\mathbf{U}^{(i-1)} - \frac{12}{\Delta t^2}{}^{t+\Delta t/2}\mathbf{U} + \frac{3}{\Delta t^2}{}^{t}\mathbf{U} - \frac{4}{\Delta t}{}^{t+\Delta t/2}\dot{\mathbf{U}} + \frac{1}{\Delta t}{}^{t}\dot{\mathbf{U}}\right) \\ &- \mathbf{C}\left(\frac{3}{\Delta t}{}^{t+\Delta t}\mathbf{U}^{(i-1)} - \frac{4}{\Delta t}{}^{t+\Delta t/2}\mathbf{U} + \frac{1}{\Delta t}{}^{t}\mathbf{U}\right) \end{aligned} \tag{24} $$

and

$$ {}^{t+\Delta t}\mathbf{U}^{(i)} = {}^{t+\Delta t}\mathbf{U}^{(i-1)} + \Delta\mathbf{U}^{(i)} \tag{25} $$

We again iterate until convergence has been achieved. The tangent stiffness matrices ${}^{t+\Delta t/2}\mathbf{K}$ and ${}^{t+\Delta t}\mathbf{K}$ used in Eqs. ( 20) and (24) with the iteration counter ($i$-1) are of course the 'consistent' tangent stiffness matrices. Here, large deformations and inelastic response can directly be included [3]. Also, contact conditions can directly be accounted for always considering only the conditions at the discrete times used above.

This scheme is a fully implicit second-order accurate method and requires per step about twice the computational effort as the trapezoidal rule. However, the accuracy per time step is significantly increased, and in particular the method remains stable when the trapezoidal rule fails to give the solution. We use this scheme as an option in nonlinear dynamics of solids and structures, and also in fluid-structure interaction solutions. In this case the first-order fluid flow equations are integrated using equations (17) and (18), of course, for velocities. The Navier-Stokes and structural finite element equations are fully coupled in the solutions, and are either solved iteratively or directly using this time integration scheme [18,19].

Since the finite element discretizations are the same in explicit and implicit dynamic solutions, restarts from explicit to implicit solutions, and vice versa, are directly possible. This option can be of use when an initially fast transient response is followed by a slow transient, almost static response. For example, in the analysis of metal forming problems, the initial

response might be well calculated using the explicit solution scheme, and the spring-back might be best calculated using the implicit scheme.

## 8. MEASURING THE SOLUTION ERROR

Assuming that the finite element solution of a mathematical model has been obtained, ideally, we could assess the solution error. Much research has focused on the 'a posteriori' assessment of these errors [21,22]. However, the problem is formidable since the error between the numerical solution and the unknown exact solution of the mathematical model shall be established.

A review of techniques has been published in Ref. [22] where it was concluded that no technique is currently available that establishes, using a given finite element solution, lower and upper bounds proven to closely bracket the exact solution, when considering general analysis, in particular nonlinear transient analysis, and an acceptable computational effort. The simple recovery-based error 'estimators' are still, in many regards, most attractive. However, they only give an indication of the error and need to be used with care.

Considering recovery-based estimators, in our experience, the stress bands proposed by Sussman and Bathe [23] (see also Ref. [3]) are quite effective to obtain error estimates in general analyses. But in practical engineering analysis, frequently very fine meshes are used, simply to ensure that an accurate solution is obtained. Then no error assessment is deemed necessary.

The recovery-based error estimators can be used directly to estimate the error in different regions of the domain analyzed. However, it may be of interest to control the error in only a specific quantity, like the bending moment at a section of the structure. In these cases, the concept of goal-oriented error estimation can be very effective and has considerable potential for further developments [21,24].

## 9. SOME ILLUSTRATIVE SOLUTIONS

The objective in this section is to briefly give some example solutions that demonstrate some of the solution characteristics described above.

### 9.1 Analyses of 360 degree rotation pendulum and rotating plate

Here we consider two problems of large deformation long time duration response, namely the the pendulum problem in Figure 1, and the rotating plate problem of Figure 2.

The analytical rotational period of the pendulum is 2.4777 sec. The solution is to be obtained for many cycles of pendulum rotation. Figure 3 shows the calculated response with the scheme of Ref. [20]. A very accurate solution has been calculated with a reasonable time step, and the solution is still acurate even after about 400 cycles. Additional results are presented in Ref. [20]

The solution of the rotating plate problem was already given in Ref. [25]. Figures 4 and 5 show the calculated response. We see that even using a rather small time step, the trapezoidal rule becomes unstable. However, the scheme of Ref. [20] remains stable even when a relatively large time step is used.

### 9.2 Analysis of 3D compound pendulum

The use of glueing of different meshes in nonlinear dynamic analyses is illustrated in Figures 6 and 7 in the analysis of a compound pendulum. The structure is subjected to an impulse. The glueing of the meshes used is shown in Figure 6 and the calculated response is given in Figure 7.

.

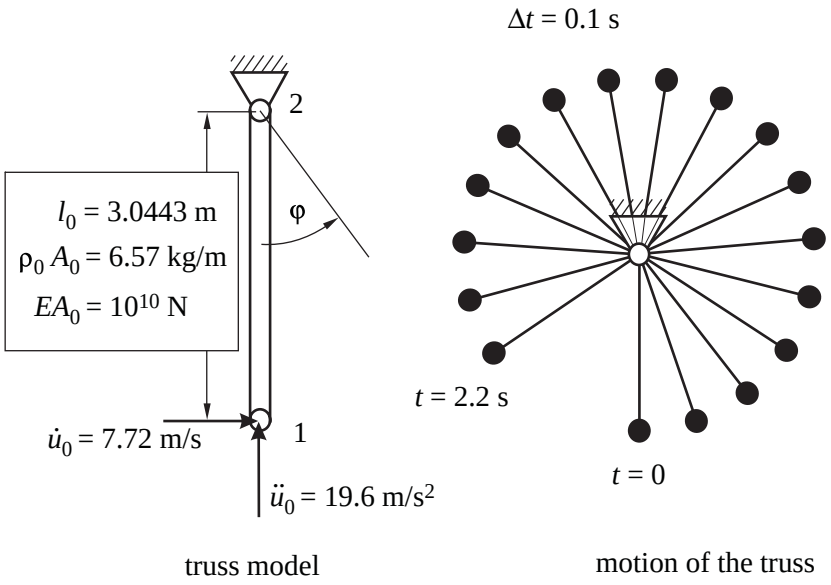


Figure 1. Simple 360 degree rotation pendulum; boundary and initial conditions

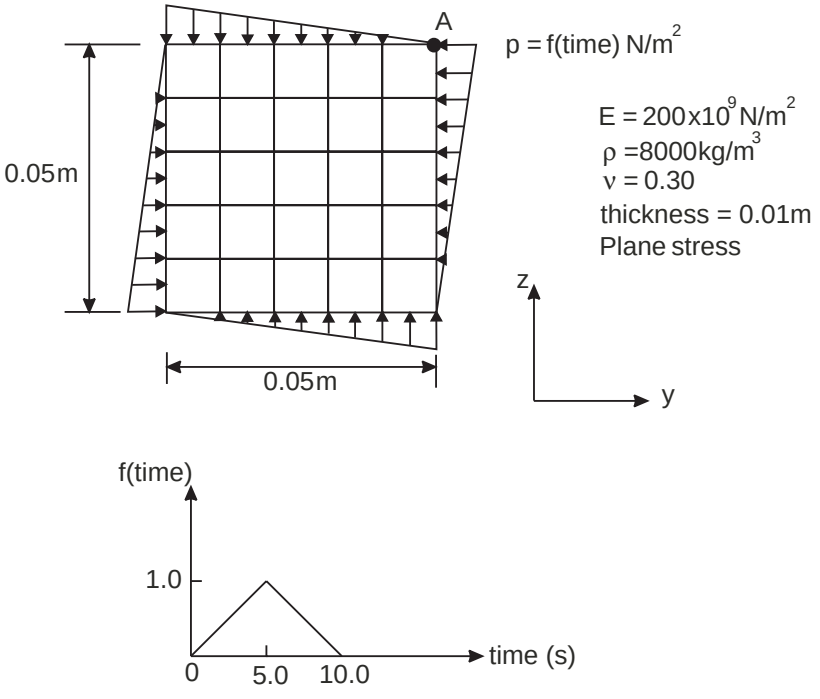


Figure 2. The rotating plate problem

The capability illustrated in Figure 6 is very important in practice because different meshes can be established for different components of a structure that are then glued together and solved for the linear or nonlinear response. The capability is also very useful in multi-scale solutions.

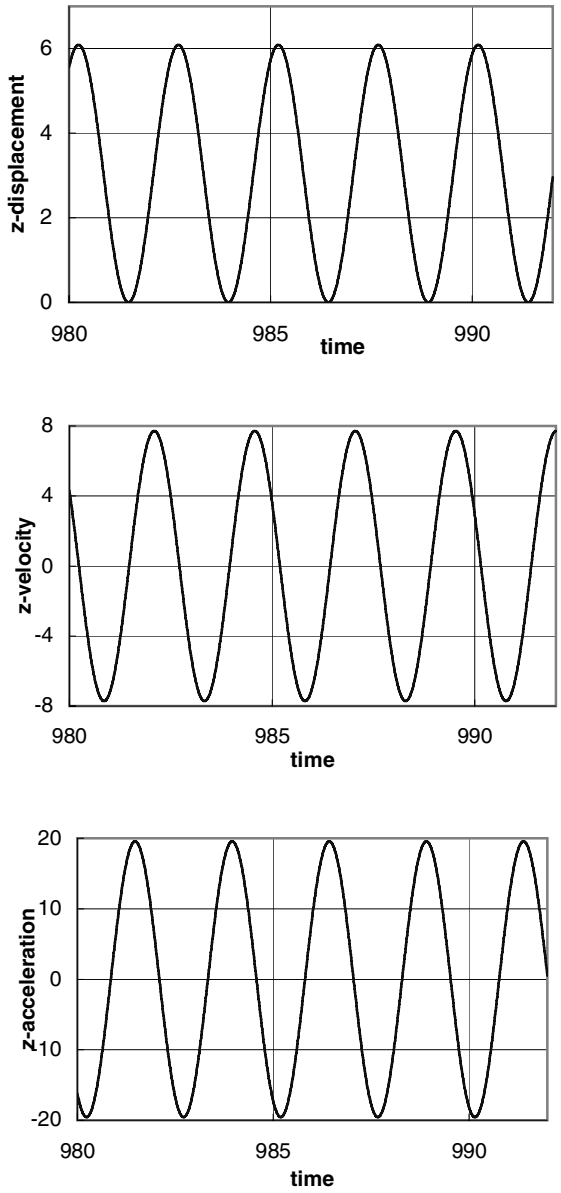


Figure 3. 360 degree rotation pendulum in 400 cycles using the scheme of Ref. [20] with $\Delta t = 0.01$

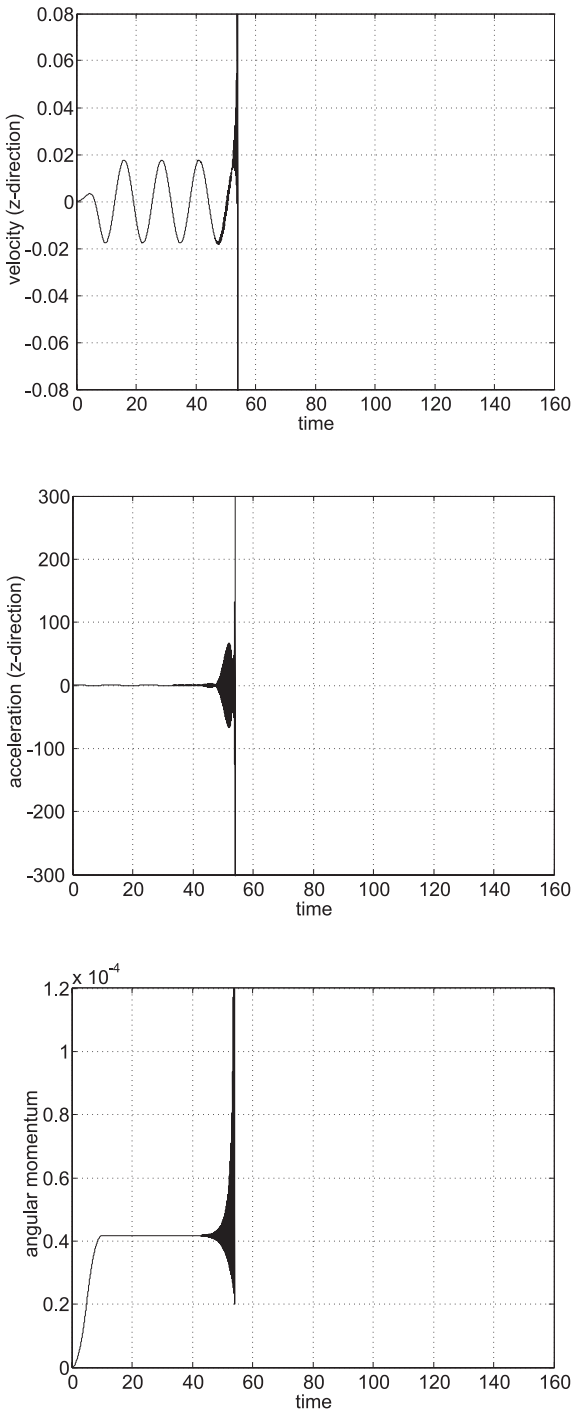


Figure 4. The rotating plate problem — results using the trapezoidal rule with $\Delta t = 0.02$ s

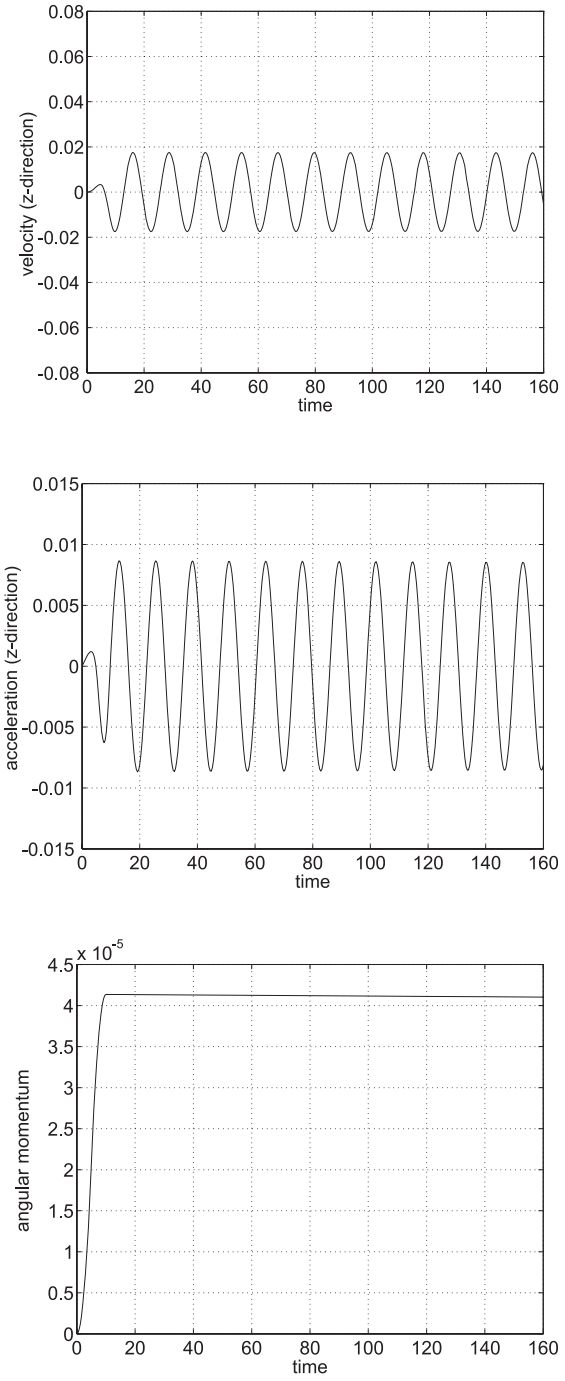


Figure 5. The rotating plate problem — results using the scheme of Ref. [20] with $\Delta t = 0.4$ s

.

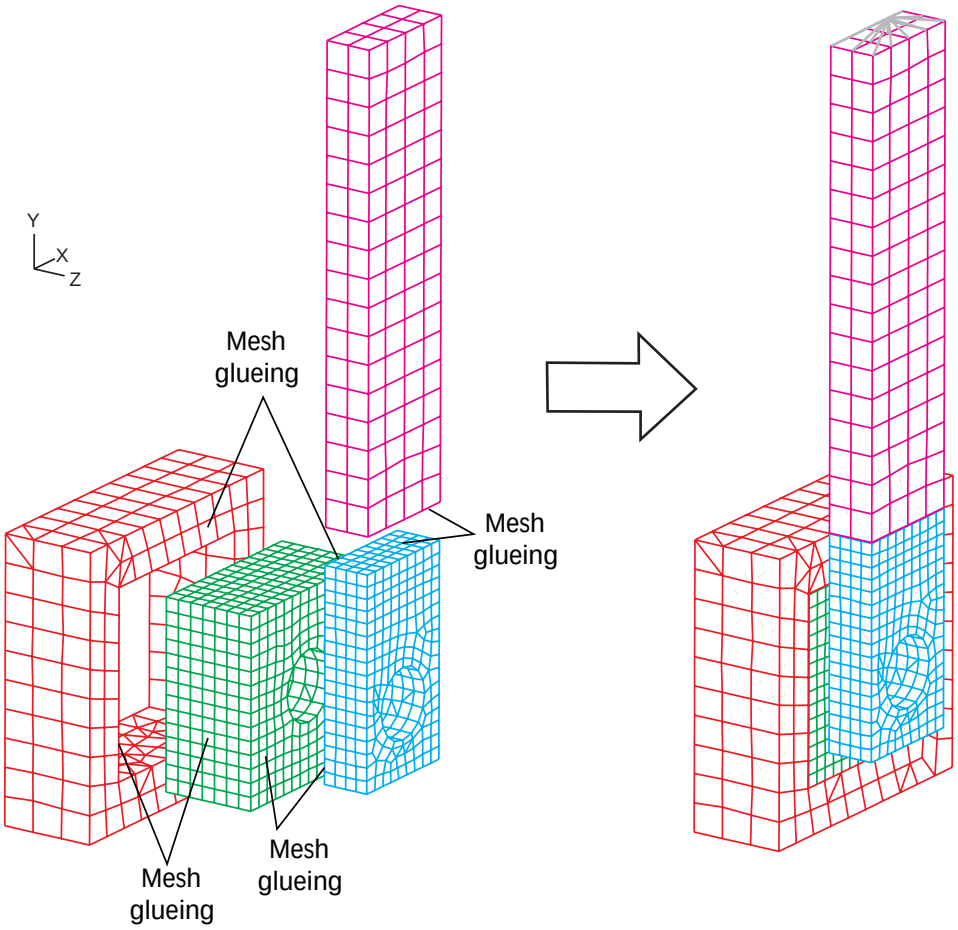


Figure 6. Glueing of meshes to model a compound pendulum using ADINA

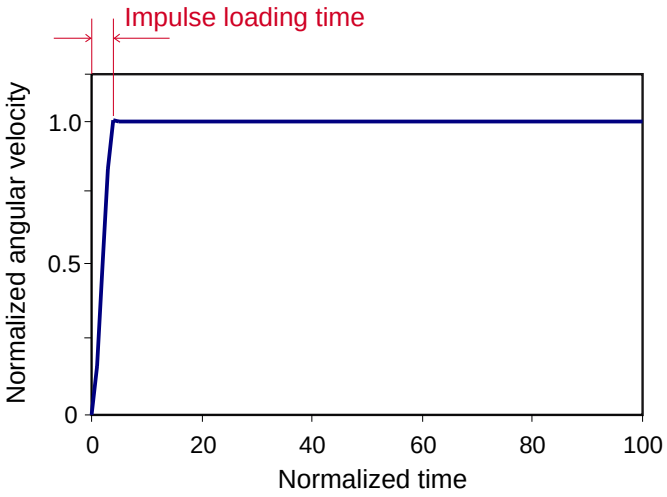


Figure 7. The calculated tip displacement of the compound pendulum

## 9.3 Analysis of shock absorber

The analysis of shock absorbers involves fluid-structure interactions in which parts of the structure and the fluid undergo very large deformations. The fluid needs to be modeled as a Navier-Stokes fluid.

Figures 8 to 10 show a shock absorber, the fluid mesh contained in the structure, and some calculated response. The fluid mesh has an initial length of about 3.2 inches and is compressed to about 0.7 inch. As the fluid is being compressed by the structure (due to the applied shock in an experiment), it exits at the bottom through openings, in stages, which causes the wavy response of the total load carried.

We see that even with the relatively coarse mesh used, the predicted load carried compares quite well with the experimental results.

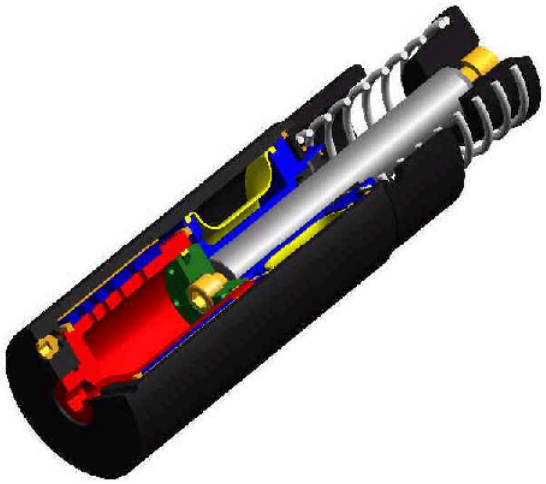

Figure 8. Shock absorber — cutaway

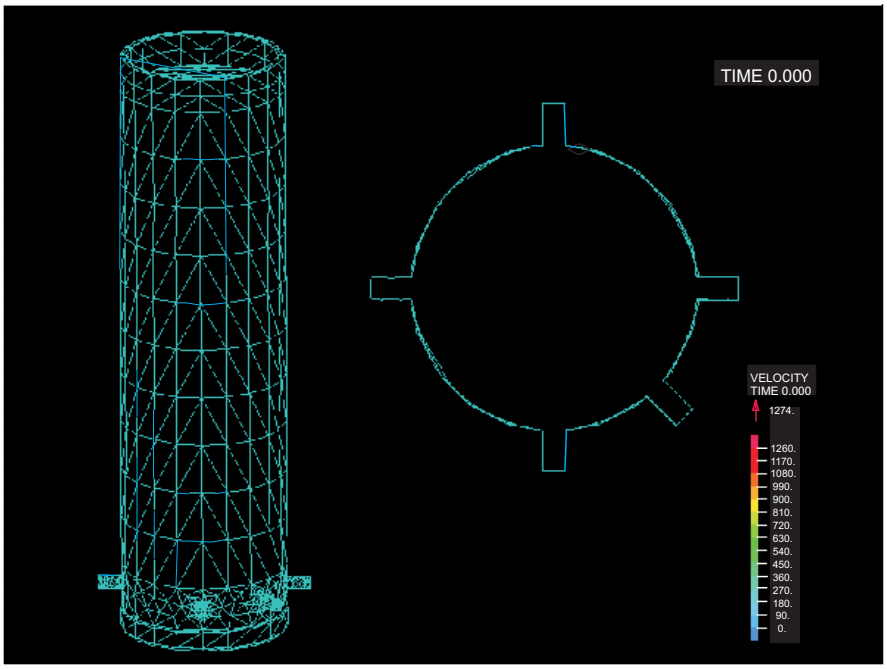


Figure 9. Fluid mesh in shock absorber

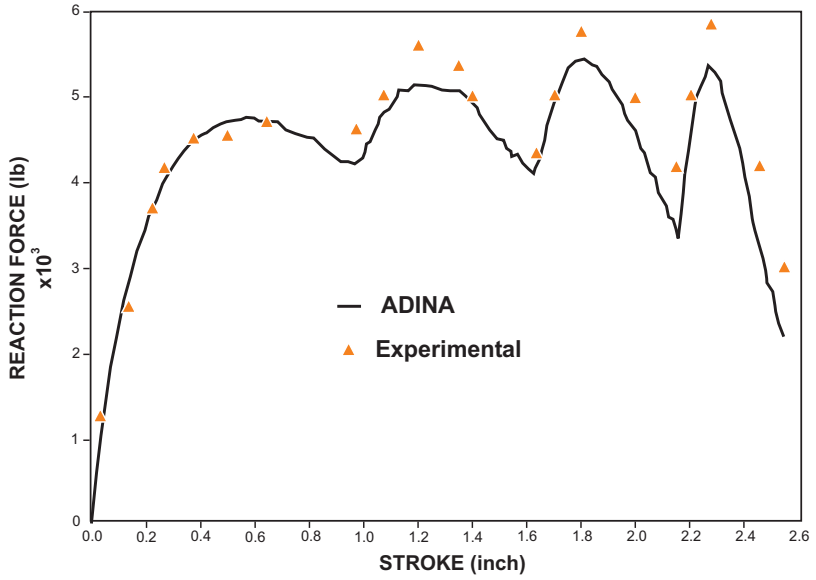


Figure 10. Shock absorber — response

## 9.4 Analysis of fuel pump

Figure 11 shows the fuel pump analyzed. Due to the vertical cam motion the diaphragm is being pushed up and down, which causes fluid to be sucked in and pushed out through the valves. These therefore have to open and close. The diaphragm and the valves are of course modeled as elastic solid media.

Figures 12 to 14 show some calculated response. In particular, Figure 14 shows that the calculated mass flow is quite close to the experimentally measured data.

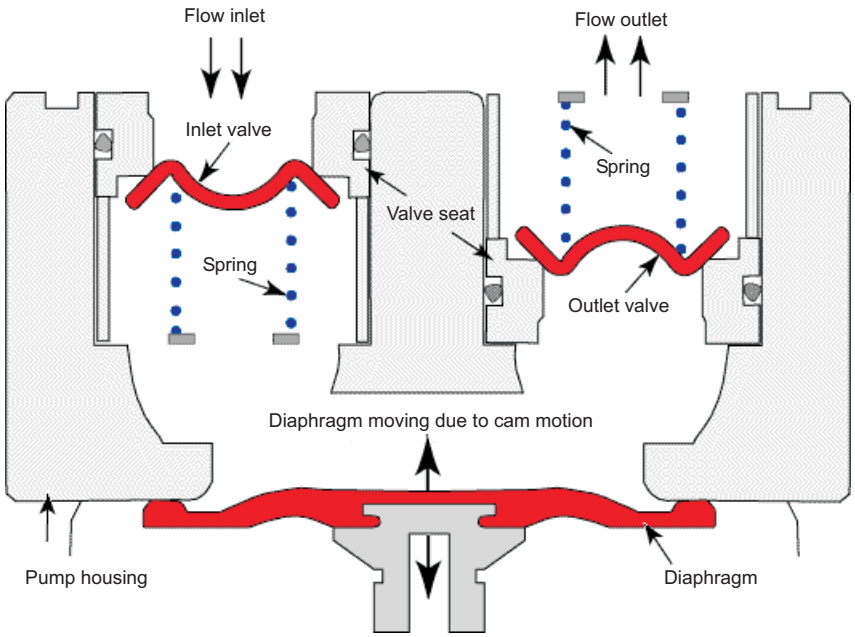


Figure 11. Fuel pump — schematic

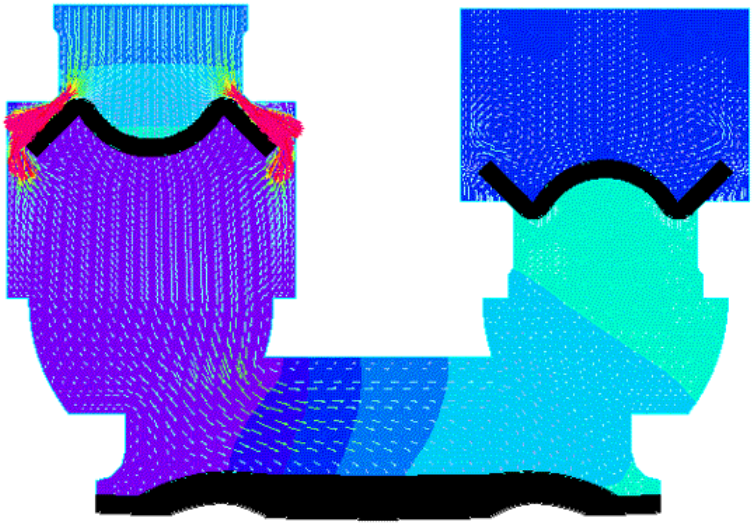

Figure 12. Fuel pump — inlet valve is open; pressure and velocity vectors; fuel flows into the chamber

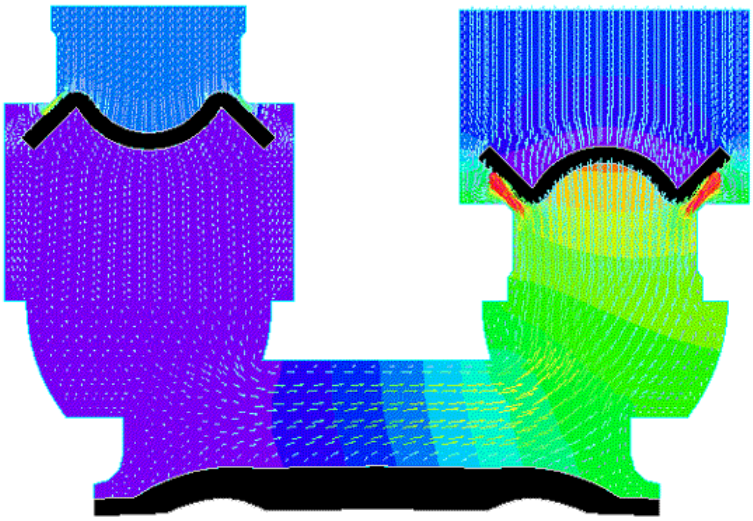

Figure 13. Fuel pump — outlet valve is open; pressure and velocity vectors; fuel flows out of the chamber

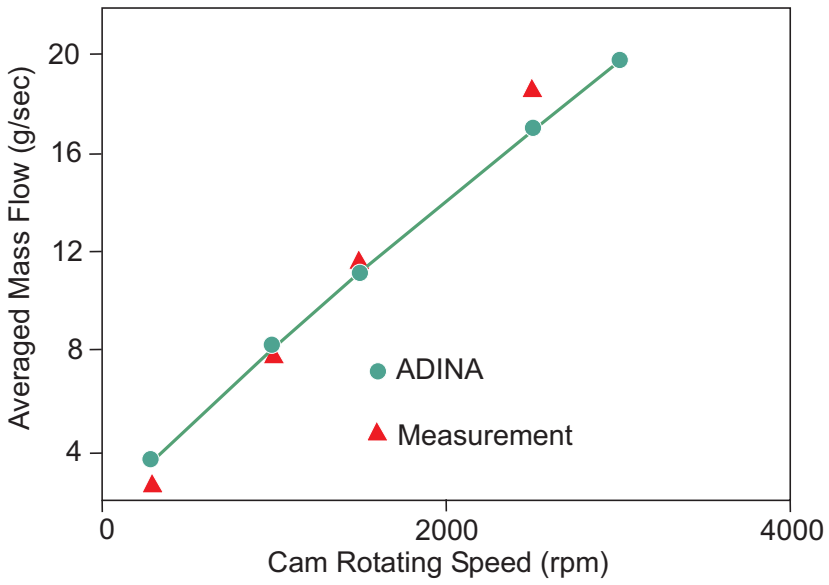


Figure 14. Fuel pump — comparison of ADINA result with measurement

## 10. CONCLUDING REMARKS

The objective in this paper was to present some developments regarding the nonlinear dynamic analysis of structures. The focus in the paper is on the need to use reliable finite element methods for such simulations. Test or field data are usually scarce, and the nonlinearity implies that measured data from even apparently similar laboratory or field test scenarios may not be of use for comparison. Hence, it is important to have as high a confidence as possible in the computed results. Such confidence, however, is only possible if reliable finite element methods are used.

The complete analysis requires the choice of a mathematical model, the finite element discretization of the model, and the time integration solution. In each of the finite element solution steps, methods should be employed that do not use adjustable parameters, that are theoretically well-founded, and known to perform reliably and effectively.

Some illustrative solutions have been presented in the paper, for additional solutions we refer to the references given, and also Refs. [26-28].

## REFERENCES

[1] K.J. Bathe, (ed.), *Computational Fluid and Solid Mechanics 2001, 2003, 2005, 2007*. Elsevier 2001, 2003, 2005, 2007.

[2] O.C. Zienkiewicz and R.L. Taylor, *The Finite Element Method*. Butterworth-Heinemann, 2005.

[3] K.J. Bathe, *Finite Element Procedures*. Prentice Hall, 1996.

[4] K.J. Bathe, On Reliable Finite Element Methods for Extreme Loading Conditions. Chapter in *Extreme Man-made and Natural Hazards in Dynamics of Structures*, A. Ibrahimbegovic and I. Kozar, eds., Springer-Verlag, 2007.

[5] F. Brezzi and M. Fortin, *Mixed and Hybrid Finite Element Methods.* Springer Verlag, New York, 1991.

[6] K.J. Bathe, The inf-sup condition and its evaluation for mixed finite element methods, *Computers & Structures*, **79**:243-252, 971, (2001).

[7] D. Pantuso and K.J. Bathe, A four-node quadrilateral mixed-interpolated element for solids and fluids, *Mathematical Models and Methods in Applied Sciences*, **5**(8):1113-1128, (1995).

[8] D. Chapelle and K.J. Bathe, *The Finite Element Analysis of Shells – Fundamentals*. Springer, 2003.

[9] D. Chapelle and K.J. Bathe, Fundamental considerations for the finite element analysis of shell structures, *Computers & Structures*, **66**(1):19-36, (1998).

[10] J. F. Hiller and K.J. Bathe, Measuring convergence of mixed finite element discretizations: an application to shell structures, *Computers & Structures*, **81**:639-654, (2003).

[11] D.N. Kim and K.J. Bathe, A 4-node 3D-shell element to model shell surface tractions and incompressible behavior, *Computers & Structures*, to appear.

[12] N. Elabbasi and K.J. Bathe, Stability and patch test performance of contact discretizations and a new solution algorithm, *Computers & Structures*, **79**:1473-1486, (2001).

[13] X. Wang and K.J. Bathe, Displacement/pressure based mixed finite element formulations for acoustic fluid-structure interaction problems, *Int. Journal for Numerical Methods in Engineering*, **40**:2001-2017, (1997).

[14] T. Sussman and J. Sundqvist, Fluid-structure interaction analysis with a subsonic potential-based fluid formulation, *Computers & Structures*, **81**:949-962, (2003).

[15] K.J. Bathe and H. Zhang, A Flow-Condition-Based Interpolation finite element procedure for incompressible fluid flows, *Computers & Structures*, **80**:1267-1277, (2002).

[16] H. Kohno and K.J. Bathe, A Flow-Condition-Based Interpolation finite element procedure for triangular grids, *Int. J. Num. Meth. in Fluids*, **51**:673-699, (2006).

[17] B. Banijamali and K.J. Bathe, The CIP method embedded in finite element discretizations of incompressible flows, *Int. Journal for Numerical Methods in Engineering*, **71**, 66-80, (2007).

[18] K.J. Bathe and H. Zhang, Finite element developments for general fluid flows with structural interactions, *Int. Journal for Numerical Methods in Engineering*, **60**:213-232, (2004).

[19] S. Rugonyi and K.J. Bathe, On the finite element analysis of fluid flows fully coupled with structural interactions, *Computer Modeling in Engineering & Sciences*, **2**:195-212, (2001).

[20] K.J. Bathe, Conserving energy and momentum in nonlinear dynamics: a simple implicit time integration scheme, *Computers & Structures*, **85**:437-445 (2007).

[21] M. Ainsworth and J.T. Oden, *A Posteriori Error Estimation in Finite Element Analysis*. J. Wiley & Sons, 2000.

[22] T. Grätsch and K.J. Bathe, *A posteriori* error estimation techniques in practical finite element analysis, *Computers & Structures*, **83**:235-265, (2005).

[23] T. Sussman and K. J. Bathe, Studies of finite element procedures — on mesh selection, *Computers & Structures*, **21:**257-264, (1985).

[24] T. Grätsch and K. J. Bathe, Goal-oriented error estimation in the analysis of fluid flows with structural interactions, *Comp. Meth. in Applied Mech. and Eng.*, **195**: 5673-5684, (2006).

[25] K.J. Bathe and M.M.I. Baig, On a composite implicit time integration procedure for nonlinear dynamics, *Computers & Structures*, **83**:2513 – 2534, (2005).

[26] K.J. Bathe, The Finite Element Method, Chapter in *Encyclopedia of Computer Science and Engineering*, J. Wiley, in press.

[27] K.J. Bathe and G.A. Ledezma, Benchmark problems for incompressible fluid flows with structural interactions, *Computers & Structures*, **85**: 628-644, (2007).

[28] http://www.adina.com/newsgrp